Journal of Physics: Conference Series **1332** (2019) 012012 doi:10.1088/1742-6596/1332/1/012012

Energetic Particle Acceleration in Shearing Flows

Frank M. Rieger[1,2]

[1] Zentrum für Astronomie (ZAH), Institut für Theoretische Astrophysik, Universität Heidelberg, Philosophenweg 12, 69120 Heidelberg, Germany
[2] Max-Planck-Institut für Kernphysik, P.O. Box 103980, 69029 Heidelberg, Germany

E-mail: f.rieger@uni-heidelberg.de

Abstract. Shear flows are ubiquitously present in space and astrophysical plasmas, and are known to be conducive to the acceleration of energetic charged particles. In particular, for relativistic flow speeds, efficient Fermi-type particle acceleration can be achieved, capable of producing momentum power-law particle distributions and sustaining energetic particles all along the shear. This paper reviews some of the key results concerning the stochastic acceleration of energetic particles in gradual shear flows and reports on some recent developments in the field.

1. Introduction

Shear flows are naturally expected in astrophysical environments; prominent examples include the rotating accretion flows around compact objects and the relativistic outflows (jets) in gamma-ray bursts (GRBs) or Active Galactic Nuclei (AGN) [1]. From a phenomenological point of view the latter have turned out to be particularly interesting. Spatially, the fast jets of powerful AGN can extend over several hundred kilo-parsecs (kpc). Bright hot spots are formed and significant back flows induced when these jets eventually interact with the ambient medium. Often these large-scale jets appear laminar despite large fluid Reynolds numbers ($Re = \rho\, u L/\mu > 10^{20}$), see Ref. [2] for orientation. The Chandra detection of extended non-thermal X-ray emission in several of these AGN jets points to the presence of energetic charged particles that have experienced continuous acceleration within them [3–5]. The favoured electron synchrotron origin of the X-ray emission in fact implies the presence of relativistic electrons with Lorentz factors up to $\gamma \sim 10^8$, e.g. [6]. Since their synchrotron cooling timescale $t_{\rm cool} \propto 1/\gamma$ and length, $c\, t_{\rm cool}$, are very short ($\ll 1$ kpc), some efficient and distributed (re-)acceleration mechanism is required to keep electrons energized throughout these jets [7]. It seems in principle conceivable that the same mechanism could also facilitate the acceleration of cosmic rays (CRs) to extreme energies, making large-scale AGN jets to possible ultra-high-energy (UHE)CR acceleration sites [8; 9].

These and other observational findings have given fresh impetus to a variety of shear particle acceleration and emission scenarios. In general, the acceleration and transport of charged particles in shearing flows can be explored on multiple scales, from the plasma skin depth (electron inertial-scale) [10] via the relativistic gyro-scale [4; 11; 12] to large turbulent length scales [13]. The present paper focuses on the second one which exhibits a history dating back to the 1980s [1; 4; 7; 11; 12; 14–26]. We will review some of the key results concerning the stochastic acceleration of energetic particles in gradual shear flows, highlight expected spectral characteristics, and report on some recent developments.

2. Basic Concept

Shear particle acceleration can be understood as a stochastic, Fermi-type [27] acceleration mechanism in which particle energization occurs as a results of elastically scattering off moving magnetic inhomogeneities [4; 28]. The energy change in an elastic scattering event is simply given by $\Delta\epsilon = \epsilon_2 - \epsilon_1 = 2\gamma_u^2(\epsilon_1 u^2/c^2 - \vec{p}_1 \cdot \vec{u})$, where $\vec{u}$ is the characteristic scattering center speed (u its magnitude, γ_u the Lorentz factor), and ϵ_1 and $\vec{p}_1$ denote the initial particle energy and momentum, respectively. Accordingly, a particle will gain energy in head-on ($\vec{p}_1 \cdot \vec{u} < 1$) collisions, and lose energy in following ($\vec{p}_1 \cdot \vec{u} < 1$) collisions. Stochastic acceleration (i.e., an average energy gain) results from the fact the interaction probability for head-on collisions is higher than the one for following collisions, retaining a second-order dependence in u, i.e., $< \Delta\epsilon > \propto (u/c)^2\epsilon$. Similarly, shear acceleration can be understood as a stochastic acceleration process, yet with the conventional scattering center speed replaced by an effective velocity u_e, given by the gradient in the flow speed multiplied by the particle free path, $\lambda = c\,\tau$. Hence, for a non-relativistic gradual shear flow with, e.g., $\vec{u} = u_z(x)\vec{e}_z$, $u_e = (\partial u_z/\partial x)\,\lambda$, and the fractional energy changes becomes

$$\frac{< \Delta\epsilon >}{\epsilon} \propto \left(\frac{u_e}{c}\right)^2 \propto \left(\frac{\partial u_z}{\partial x}\right)^2 \lambda^2. \tag{1}$$

This suggests a characteristic acceleration timescale

$$t_{\rm acc} = \frac{\epsilon}{(d\epsilon/dt)} \sim \frac{\epsilon}{< \Delta\epsilon >} \times \frac{\lambda}{c} \;\propto\; \frac{1}{\lambda}\,, \tag{2}$$

which, in contrast to classical 1st and 2nd order Fermi acceleration, is inversely depending on the particle mean free path. In the case of e.g. a gyro-dependence with $\lambda \sim r_g \propto \gamma$, $t_{\rm acc}$ would reveal the same scaling as the synchrotron loss timescale $t_{\rm cool}$, with interesting implications [22]. The principal reason for this unusual behaviour is related to the fact that as a particle increases its energy ($\epsilon \simeq \gamma mc^2$) and thereby its mean free path ($\lambda \propto \gamma^\alpha, \alpha > 0$), a higher effective velocity u_e is experienced. For shear to start operating efficiently within a system, one thus usually requires injection of some pre-accelerated seed particles, either from acceleration at shocks or via classical 2nd order Fermi processes [7]. The situation is typically more favourable, though, for the case of protons or ions.

3. Microscopic Picture - Fokker-Planck type diffusion for non-relativistic flows

A more detailed picture of the particle evolution becomes apparent in a microscopic approach via an explicit calculation of the average rate of momentum change and dispersion (i.e., the corresponding Fokker Planck coefficients). Consider for simplicity a non-relativistic shear flow with $\vec{u} = u_z(x)\vec{e}_z$. While travelling across the flow, the momentum of a particle relative to the flow will change by $\vec{p}_2 = \vec{p}_1 + m\,\delta\vec{u}$, where $\delta\vec{u} = (\partial u_z/\partial x)\delta x\,\vec{e}_z$ with $\delta x = v_x\,\tau$, and where the timescale for collisions (scattering time) might be a function of momentum, i.e., $\tau \equiv \tau(p) = \tau_0\,p^\alpha$. Expanding $(p_2 - p_1)$ to second order in δu and averaging over an isotropic particle distribution, the Fokker Planck coefficients then become [16; 22]

$$\begin{aligned} \left\langle \frac{\Delta p}{\Delta t} \right\rangle &\propto p \left(\frac{\partial u_z}{\partial x}\right)^2 \tau\,, \\ \left\langle \frac{(\Delta p)^2}{\Delta t} \right\rangle &\propto p^2 \left(\frac{\partial u_z}{\partial x}\right)^2 \tau\,. \end{aligned} \tag{3}$$

The Fokker Planck coefficients can be shown to be related by the equation

$$\left\langle \frac{\Delta p}{\Delta t} \right\rangle = \frac{1}{2p^2}\frac{\partial}{\partial p}\left[p^2 \left\langle \frac{(\Delta p)^2}{\Delta t} \right\rangle\right] = \frac{\Gamma}{p^2}\frac{\partial}{\partial p}\left(p^4\tau\right)\,, \tag{4}$$

i.e., to satisfy the principle of detailed balance (scattering being reversible). Here Γ in eq. (4) denotes the shear flow coefficient, and for the employed flow profile is given by $\Gamma = (1/15)(\partial u_z/\partial x)^2$. Under the condition of detailed balance, the associated Fokker-Planck equation reduces to a diffusion equation in momentum space. Hence in the absence of radiative losses, the particle phase-space distribution function $f(p,t)$ undergoing shear acceleration might be cast in a simple Fokker-Planck type diffusion equation

$$\frac{\partial f(p,t)}{\partial t} = \frac{1}{p^2}\frac{\partial}{\partial p}\left(p^2 D\,\frac{\partial f}{\partial p}\right)\,, \tag{5}$$

where D denotes the momentum space diffusion coefficient, and for the considered application is given by

$$D = \Gamma p^2 \tau = \frac{1}{15}\left(\frac{\partial u_z}{\partial x}\right)^2 p^2 \tau\,, \tag{6}$$

where $\tau = \tau_0\, p^\alpha$. Figure 1 shows an exemplary solution of eq. (5) for the case $\tau \propto p$ [22]. At

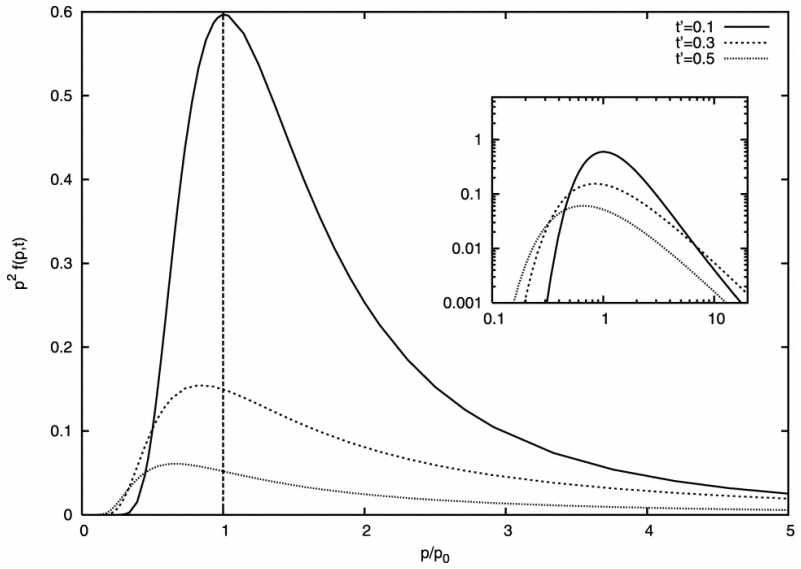

Figure 1. Time-dependent solution $f(p,t)$ of the Fokker-Planck diffusion equation for non-relativistic shear assuming (impulsive) mono-energetic injection with p_0 at $t_0 = 0$. A momentum-dependence $\alpha = 1$ has been used. The distribution broadens with time due to momentum dispersion. The inlet illustrates the formation of a power law like distribution $n(p) \propto p^2 f(p) \propto p^{-2}$ above p_0 for $t' \geq 0.3$.

sufficiently large times, the particle distribution above the injection momentum p_0 approaches a power law shape

$$n(p) \propto p^2 f(p) \propto p^{-(1+\alpha)}\,, \tag{7}$$

for $\alpha > 0$, with power law index depending on the scaling of the particle mean free path ($\lambda \simeq c\tau \propto p^\alpha$) [11; 14; 22]. In particular, for a gyro-dependence, $\alpha = 1$, one has $n(p) \propto p^{-2}$, similar to first-order Fermi acceleration at non-relativistic shocks. The quasi steady-state (time-integrated) distribution $f(p)$ for continuous injection then becomes constant below p_0, and takes on the noted power-law shape ($\propto p^{-(3+\alpha)}$) above it.

4. Non-relativistic particle transport equation

In order to take spatial transport into account, an extended particle transport equation needs to be derived. In the non-relativistic limit this has been done by Earl et al. [12], starting from the non-relativistic Boltzmann equation for the phase-space distribution $f(\vec{x},\vec{p},t)$ and assuming a simple BKG-type collision term, $(\partial f/\partial t)_s = (f - \langle f\rangle)/\tau$. The approach relies on a mixed system of phase-space coordinates such that quantities which are operated upon the scattering operator, i.e. the momentum, are evaluated in the comoving flow frame (allowing to treat the scattering physics in simple ways), while time and space coordinates are still measured in the laboratory frame. Given non-relativistic flow speeds the particle momentum components are then related by a Galilean transformation $p_i = p'_i + m\,u_i$ (background flow speed u_i, comoving p'_i). Scattering is assumed to be strong enough to guarantee the diffusion approximation, i.e., to ensure that the departure from isotropy is small, $f = f_0 + f_1$, with $< f_1 >= 0$ and $f_1 \ll f_0$. The full non-relativistic particle transport equation for $f_0(\vec{x},p',t)$ then becomes [12]

$$\begin{aligned}\frac{\partial f_0}{\partial t} + u_i\,\frac{\partial f_0}{\partial x_i} \;&-\; \frac{p'}{3}\,\frac{\partial u_i}{\partial x_i}\,\frac{\partial f_0}{\partial p'} - \frac{\partial}{\partial x_i}\left(\kappa\,\frac{\partial f_0}{\partial x_i}\right)\\ &+\; \frac{2\,\tau\,p'}{3}\,A_i\,\frac{\partial^2 f_0}{\partial x_i \partial p'} + \frac{1}{3\,p'^2}\,\frac{\partial\,(\tau\,p'^3)}{\partial p'}\,A_i\,\frac{\partial f_0}{\partial x_i}\\ &-\; \frac{\Gamma}{p'^2}\,\frac{\partial}{\partial p'}\left(\tau\,p'^4\,\frac{\partial f_0}{\partial p'}\right) + \frac{p'}{3}\,\frac{\partial(\tau A_i)}{\partial x_i}\,\frac{\partial f_0}{\partial p'} = 0\,,\end{aligned} \tag{8}$$

$(i = 1, 2, 3)$, where κ denotes the isotropic spatial diffusion coefficient, $\kappa(p) = \tau(p)c^2/3$, and

$$A_i = \frac{\partial u_i}{\partial t} + u_l\,\frac{\partial u_i}{\partial x_l} \tag{9}$$

is the viscous shear flow coefficient given by

$$\Gamma = \frac{1}{30}\left(\frac{\partial u_i}{\partial x_k} + \frac{\partial u_k}{\partial x_i}\right)^2 - \;\frac{2}{45}\,\frac{\partial u_i}{\partial x_i}\,\frac{\partial u_k}{\partial x_k}\,. \tag{10}$$

The second, third and fourth term in eq. (8) relate to the well-known effects of convection, adiabatic energy change and spatial diffusion, while the terms involving A_i describe the effects of inertial drifts (cf. also [29] for incorporation of a mean magnetic field). The additional term involving Γ characterizes the energy changes due to flow shear and divergence. For a steady (non-relativistic) shear flow of the form $\vec{u} = u_z(x)\vec{e}_z$, the adiabatic and inertial terms vanishes ($\partial u_i/\partial x_i = 0$ and $A_i = 0$), Γ reduces to $\Gamma = (1/15)(\partial u_z/\partial x)^2$, and the space-independent part of eq. (8) becomes

$$\frac{\partial f_0}{\partial t} = \frac{\Gamma}{p'^2}\,\frac{\partial}{\partial p'}\left(\tau\,p'^4\,\frac{\partial f_0}{\partial p'}\right)\,, \tag{11}$$

thus coinciding with eq. (5).

5. Relativistic Generalization

To compete with diffusive particle escape, efficient shear particle acceleration typically requires relativistic flow speeds (see also below). This then demands a generalization of the particle transport to the relativistic regime as has been obtained by e.g. Webb et al. [15; 18]. Assuming isotropic diffusion and denoting the (covariant) metric tensor by $g_{\alpha\beta}$, the zero component of the (comoving) particle momentum four vector by $p'^0 = E'/c$, the fluid four velocity by u_α and the fluid four acceleration by $\dot{u}_\alpha := u^\beta \nabla_\beta u_\alpha$, with $\nabla_\beta u_\alpha$ indicating covariant derivation, the full

particle transport equation for the isotopic distribution function $f_0(x^\alpha, p')$ with $x^\alpha = (ct, x, y, z,)$ becomes [15]

$$\nabla_\alpha \left[c u^\alpha f_0 - \kappa \left(g^{\alpha\beta} + u^\alpha u^\beta \right) \left(\frac{\partial f_0}{\partial x^\beta} - \dot{u}_\beta \frac{(p^0)^2}{p'} \frac{\partial f_0}{\partial p'} \right) \right] + \frac{1}{p'^2} \frac{\partial}{\partial p'} \left[-\frac{p'^3}{3} c \nabla_\beta u^\beta f_0 + p'^3 \left(\frac{p'^0}{p'} \right)^2 \kappa \dot{u}^\beta \left(\frac{\partial f_0}{\partial x^\beta} - \dot{u}_\beta \frac{(p'^0)^2}{p'} \frac{\partial f_0}{\partial p'} \right) - \Gamma \tau p'^4 \frac{\partial f_0}{\partial p'} \right] = Q \,, \tag{12}$$

where Q denotes the source term and Greek indices (α, β) run from 0 to 3. Γ denotes the (generalized) relativistic shear coefficient, which in the strong scattering limit is given by

$$\Gamma = \frac{c^2}{30} \sigma_{\alpha\beta} \sigma^{\alpha\beta} \,, \tag{13}$$

where $\sigma_{\alpha\beta}$ is the (covariant) fluid shear tensor. For a cylindrical jet with a steady (relativistic) shear flow profile $\vec{u} = u(r)\vec{e}_z$, the fluid four acceleration ($\dot{u}_\alpha = 0$) and divergence ($\nabla_\beta u^\beta = 0$) vanish, retaining only the shear term with $\Gamma = (\gamma_u^4/15)\,(du/dr)^2$ in the second line of eq. (12). z-independent, steady-state solutions of eq. (12) for such a flow profile and a specific form of the radial dependence of $\kappa(r, p)$ have been recently presented by Webb et al. [26].

6. Application

In the following some recent applications and results in the context of shear particle acceleration are briefly reported.

6.1. Particle acceleration in expanding flows

Both, the jets in AGN and GRBs exhibit relativistic speeds, and are likely to be (quasi-conically) expanding, motivating an analysis of particle acceleration in expanding, relativistic shear flows [21; 24]. For the simplest case of a radial shear flow profile $u^\alpha = \gamma_v\,(\theta)(1, v_r(\theta)/c, 0, 0)$, where θ denotes the polar angle and r the radial coordinate, the impact of different functional dependencies for $\gamma_v(\theta)$, i.e., a power-law-, Gaussian- or Fermi-Dirac-type can be explored, see Fig. 2. The associated characteristic (comoving) acceleration timescales for a particle with mean free path λ' [24],

$$t_{\rm acc}(r, \theta)' \sim \frac{2\,c\,r^2}{\gamma_v^2\,(v_r^2 + 0.75\,\gamma_v^2\,[\partial v_r/\partial\theta]^2)\,\lambda'} \,, \tag{14}$$

can then become a strong function of θ, allowing for the generation of some prominent non-axis emission features (e.g., 'ridge line'). To overcome adiabatic losses ($\propto \gamma_v v_r/r$) and experience efficient acceleration, relativistic flow speeds and sufficient energetic seed particles ($\lambda'/r > 10^{-3}$ for the application presented in Fig. 2) are needed. It seems possible that such a process could lead to a weak and long-duration leptonic emission component in GRBs, and facilitate cosmic-ray acceleration to ultra high energies [21].

6.2. Generating multi-component particle distributions

As a two-stage process, stochastic shear acceleration could lead to the formation of multi-component particle distributions. A basic example considering radiative-loss-limited acceleration in a mildly relativistic shearing flow is shown in Fig. 3 [7]. The figure is based on a solution of the Fokker-Planck equation for $f(p, t)$ (or equivalently, $f(\gamma, t)$) including classical 2nd order Fermi and shear particle acceleration as well as radiative synchrotron losses. Employing a mean

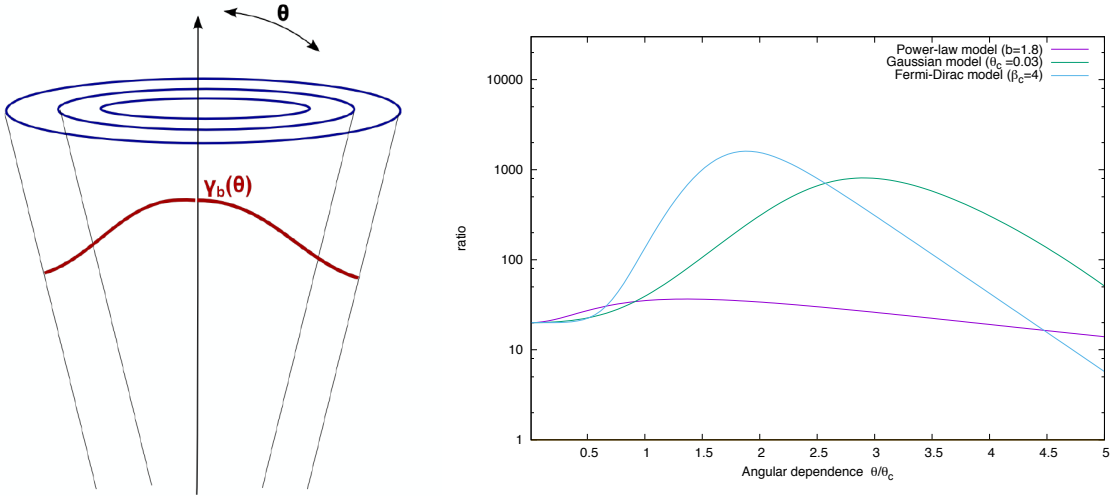

Figure 2. Left: Illustration of a simple radially expanding flow. Right: Ratio of viscous shear gain versus adiabatic losses multiplied by (r/λ'), illustrated for $\theta_c = 0.03$ rad and a flow Lorentz factor $\gamma_v = 30$ on the axis [24]. A non-axis preference becomes particularly evident for a Gaussian or Fermi-Dirac shaped flow profile.

free path scaling $\lambda = \xi^{-1} r_g \, (r_g/\Lambda_{\rm max})^{1-q} \propto \gamma^{2-q}$, with $q = 5/3$ (Kolmogorov) and $\xi = 0.1$, and choosing parameters applicable to the large-scale jets in AGN, electron acceleration up to Lorentz factors $\gamma \sim 10^9$ seems feasible. Stochastic 2nd order Fermi acceleration dominates particle energization up to $\gamma \sim 10^4$ above which efficient shear acceleration becomes operative leading to a somewhat flatter spectral slope (changing by 2/3 for the noted application). Synchrotron radiation eventually introduces a spectral cut-off at high energies. As shearing conditions are likely to prevail along astrophysical jets, these findings illustrate that the considered processes could be of relevance for understanding the extended X-ray emission in the large-scale jet of AGN (cf. Sec 1). Moreover, by the same means relativistic large-scale AGN jets could also facilitate the acceleration of cosmic rays to ultra-high energies [7; 26].

6.3. Spatial transport and diffusive escape

The above considerations did not account for details of the spatial transport, and possible modifications introduced by the diffusive escape of particles from the system. Implications of these could in principle be analyzed with resort to the relativistic particle transport equation (12). Deriving analytical, steady-state solutions $f_0(r, p')$ for a cylindrical jet, assuming z-independence and a special form for the radial dependence of the scattering time, $\tau(r, p) = \tau_0 \, (p/p_0)^\alpha / [r \, d\xi(r)/dr]$ where $\xi(r) \equiv 0.5 \ln(1 + \beta(r)/[1 - \beta(r)])$, with $\beta(r) = u(r)/c$ the flow speed, Webb et al. [26] showed that diffusive escape could counter-act efficient acceleration. While the local particle distribution still follows a power law $f(p') \propto p'^{-\mu}$, its momentum index μ becomes dependent on the maximum flow speed β_0 on axis, and significantly steepens with decreasing β_0 (with $\mu \to \infty$ for $\beta_0 \to 0$). Though possible limitations due to the chosen τ-dependence may deserve some further studies, these results imply that efficient shear particle acceleration requires relativistic flow speeds. This becomes also apparent when comparing the corresponding timescale for acceleration, $t'_{\rm acc} \sim 1/[\gamma_u^4 (du/dr)^2 \tau']$, with the one for cross-field escape $t'_e \sim r^2/[c^2 \tau']$.

The analytical solutions [26] can be used to gain insights into the radial evolution of the particle transport. Below an example is given for the particle transport in the presence of a

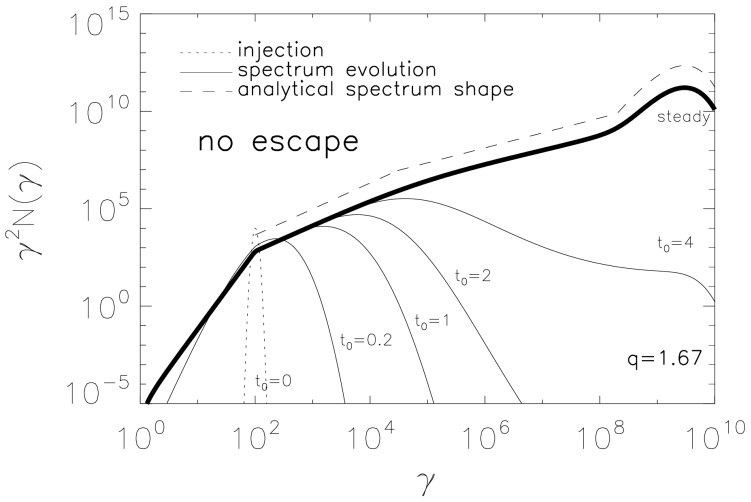

Figure 3. Time-evolution of the electron spectrum $\gamma^2\, n(\gamma)$ in the presence of stochastic-shear particle acceleration, where $n(\gamma) \propto \gamma^2 f(\gamma)$ represents a solution of the corresponding Fokker Planck equation given a linearly decreasing shear flow profile of width $\Delta r \sim r_j/10$ and an Alfven speed $\beta_A \sim 0.007$ [7]. Above particle Lorentz factors of a few times 10^4 the spectrum is shaped by shear acceleration, with a high-energy spectral cut-off around $\gamma \sim 10^9$ being introduced by synchrotron losses.

hyperbolic, relativistic shear flow as shown in Fig. 4.

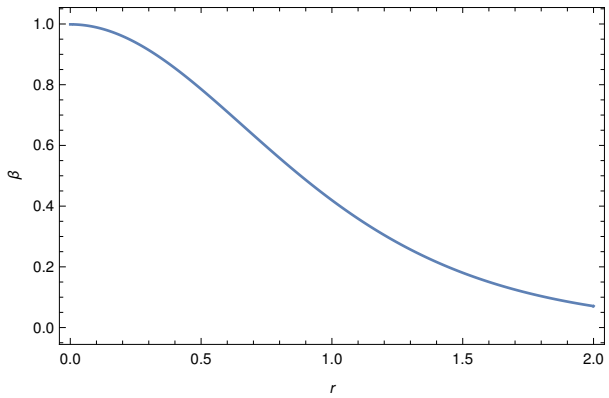

Figure 4. Relativistic flow profile $\beta(r)\,\vec{e}_z$ chosen for evaluating the particle distribution function in Fig. 5. A maximum flow Lorentz factor $\gamma_\beta = 20$ on the axis has been assumed.

Figure 5 provides an illustration that away from injection the 'classical' power-law momentum dependence, eq. (7), is recovered at high flow speeds ($\beta_0 \to 1$). Clearly, advancing our understanding of the (radial) diffusion properties in astrophysical jets will be important to better characterize the efficiency of shear particle acceleration.

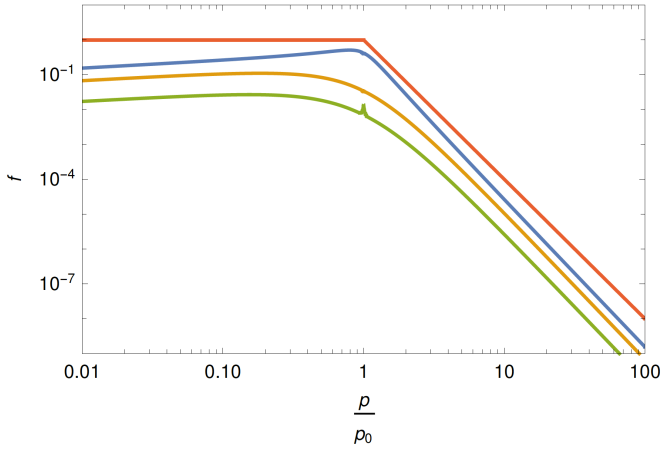

Figure 5. Steady-state solution $f(r, p')$ as a function of momentum p'/p'_0 for the flow profile in Fig. 4 and three different spatial locations, $r = 0.06$ (blue), $r = 0.50$ (orange), $r = 1.20$ (green). Mono-energetic particle injection with p'_0 at $r_1 = 0.02$ and an outer (escape) boundary at $r_2 = 2$ have been assumed. A momentum-dependence of $\alpha = 1$ has been employed for the scattering time. The red curve (top) designates the classical power-law dependence, with $f(p') \propto p'^{-4}$ above p'_0, as inferred from the Fokker-Planck approach in Sec. 3.

7. Conclusions

Particle acceleration in fast shearing flows could represent a promising mechanism for the continued acceleration of charged particles, capable of producing (local) power-laws in momentum. As such it can provide a plausible explanation for, e.g., the origin of the extended high-energy emission seen in the large-scale jets of AGN, and contribute to the energization of extreme cosmic rays.

In many circumstances, injection of energetic seed particles (in the case of electrons) and relativistic flow speeds will be required for the mechanism to operate efficiently. In the case of AGN and GRBs the former condition are likely to be met by first-order shock and/or stochastic second-order Fermi processes. In this regard, shear acceleration thus resembles a two-stage process for facilitating particle acceleration beyond the common limit.

To further improve our understanding, high-resolution studies of astrophysical jets and a quantitative analysis of the stability and radial transport properties of fast shearing flows are of particular interest.

Acknowledgments

I would like to thank Gary Zank and the organizers for the invitation to an inspiring and pleasant 18th AIAC conference. I am also grateful to Peter Duffy, Felix Aharonian and Ruoyu Liu for collaboration and discussion. Financial support by a DFG Heisenberg Fellowship under RI 1187/6-1 is acknowledged.

References

[1] Rieger F M and Duffy P 2004 *ApJ* **617** 155–161 (*Preprint* `astro-ph/0410269`)

[2] Worrall D M and Birkinshaw M 2006 *Physics of Active Galactic Nuclei at all Scales* (*Lecture Notes in Physics, Berlin Springer Verlag* vol 693) ed Alloin D p 39 (*Preprint* `astro-ph/0410297`)

[3] Harris D E and Krawczynski H 2006 *ARA&A* **44** 463–506 (*Preprint* astro-ph/0607228)
[4] Rieger F M, Bosch-Ramon V and Duffy P 2007 *Ap&SS* **309** 119–125 (*Preprint* astro-ph/0610141)
[5] Georganopoulos M, Meyer E and Perlman E 2016 *Galaxies* **4** 65
[6] Sun X N, Yang R Z, Rieger F M, Liu R Y and Aharonian F 2018 *A&A* **612** A106 (*Preprint* 1712.06390)
[7] Liu R Y, Rieger F M and Aharonian F A 2017 *ApJ* **842** 39 (*Preprint* 1706.01054)
[8] Aharonian F A, Belyanin A A, Derishev E V, Kocharovsky V V and Kocharovsky V V 2002 *Phys. Rev. D* **66** 023005 (*Preprint* astro-ph/0202229)
[9] Kotera K and Olinto A V 2011 *ARA&A* **49** 119–153 (*Preprint* 1101.4256)
[10] Alves E P, Grismayer T, Fonseca R A and Silva L O 2014 *New Journal of Physics* **16** 035007 (*Preprint* 1404.0555)
[11] Berezhko E G and Krymskii G F 1981 *Soviet Astronomy Letters* **7** 352
[12] Earl J A, Jokipii J R and Morfill G 1988 *ApJL* **331** L91–L94
[13] Ohira Y 2013 *ApJL* **767** L16 (*Preprint* 1301.6573)
[14] Berezhko E G 1982 *Soviet Astronomy Letters* **8** 403–405
[15] Webb G M 1989 *ApJ* **340** 1112–1123
[16] Jokipii J R and Morfill G E 1990 *ApJ* **356** 255–258
[17] Ostrowski M 1990 *A&A* **238** 435–438
[18] Webb G M, Jokipii J R and Morfill G E 1994 *ApJ* **424** 158–180
[19] Rieger F M and Mannheim K 2002 *A&A* **396** 833–846 (*Preprint* astro-ph/0210286)
[20] Ostrowski M 1998 *A&A* **335** 134–144 (*Preprint* astro-ph/9803299)
[21] Rieger F M and Duffy P 2005 *ApJL* **632** L21–L24 (*Preprint* astro-ph/0509495)
[22] Rieger F M and Duffy P 2006 *ApJ* **652** 1044–1049 (*Preprint* astro-ph/0610187)
[23] Dempsey P and Rieger F M 2009 *International Journal of Modern Physics D* **18** 1651–1654
[24] Rieger F M and Duffy P 2016 *ApJ* **833** 34 (*Preprint* 1611.04342)
[25] Kimura S S, Murase K and Zhang B T 2018 *Phys. Rev. D* **97** 023026 (*Preprint* 1705.05027)
[26] Webb G M, Barghouty A F, Hu Q and le Roux J A 2018 *ApJ* **855** 31
[27] Fermi E 1949 *Physical Review* **75** 1169–1174
[28] Lemoine M 2019 *arXiv e-prints* (*Preprint* 1903.05917)
[29] Williams L L and Jokipii J R 1991 *ApJ* **371** 639–647